scientific reports

Check for updates

OPEN

Modal test and finite element updating of sprayer boom truss

Qi Chen, Shaohao Zhou, Yuanfeng Xiao, Linfeng Chen, Yang Zhou & Lihua Zhang✉

In addressing the finite element model and actual structural error of the sprayer boom truss, this study aims to achieve high-precision dynamic characteristics, enhance simulation credibility, make informed optimization decisions, and reduce testing costs. The research investigates the dynamic behavior of the sprayer boom truss through modal experiments and finite element simulations. Initially, modal parameters of the sprayer boom are obtained through experimental testing, validating their reasonableness and reliability. Subsequently, Ansys Workbench18.0 simulation software was employed to analyze the finite element model of the sprayer boom, revealing a maximum relative error of 11.93% compared to experimental results. To improve accuracy, a kriging-based response surface model was constructed, and multi-objective parameter adjustments using the MOGA algorithm reduce the maximum relative error to 4.6%. Sensitivity analysis further refines the model by optimizing target parameters, resulting in a maximum relative error of 4.96%. These findings demonstrate the effective enhancement of the corrected finite element model's precision, with the response surface method outperforming sensitivity analysis the maximum relative error between the updated finite element model and experimental results was within the engineering allowable range, confirming the effectiveness of the updated model.

Keywords Spray boom, Finite element analysis, Modal experiment, Model updating

The spray boom of a sprayer is a crucial component for ensuring the quality of spraying operations. To enhance the uniformity of spray deposition, structural optimization and vibration reduction of the spray boom have significant research and practical value[1–4]. Iterative optimization based on experimental results of the actual structure is reliable and realistic. However, the long production cycle, high cost, and difficulty in setting up test environments pose challenges[5,6]. In response to these issues, finite element simulation software has emerged, improving analysis efficiency and reducing development costs. However, numerical models analyzed using finite element simulation software often exhibit significant differences from the measured values in actual experiments, leading to incorrect results and providing misguided guidance for optimization[7,8]. To obtain more accurate dynamic characteristics of the model, it is crucial to establish a finite element model that matches the experimental data. The inaccuracies in finite element models generally arise from structural errors, order errors, and parameter errors[9]. The first two errors can be reduced by improving the model's accuracy. Parameter errors usually result from inaccurate estimates of materials, geometric parameters, connections, and boundary conditions. A finite element model updated based on experimental data exhibits higher accuracy and can provide meaningful guidance for subsequent optimization designs[10].

Currently, updating of model parameter errors is a mainstream research direction. Xu et al.[11] conducted modal experiments to correct the density, elastic modulus, and bow head spring stiffness of the pantograph. The final experimental results showed a simulation error of 5.2%. He et al.[12], focusing on helical bevel gears, used modal experiments to target test parameters. They constructed a quadratic response surface model to correct finite element model parameters, thereby improving model accuracy. Other scholars have also employed various methods for model parameter updating. Liu et al.[13] improved the glow-worm algorithm to correct both simply supported beam and rigid frame bridge models, significantly reducing frequency errors and verifying the superiority of the algorithm. Li et al.[14], Zhang et al.[15], both utilized kriging models for model updating on different research subjects, resulting in improved model accuracy. Sensitivity analysis has proven effective in enhancing updating efficiency. Su et al.[16], Liu et al.[17], Zhang et al.[18], and Mottershead et al.[19] all applied sensitivity analysis methods for model parameter updating, demonstrating that this approach consistently achieved accurate models.

This article employs modal experiments to extract the modal parameters of the spray boom, and the simulation is carried out, and the simulation parameters are compared and analyzed with the test parameters. A central composite experiment is designed for material density, Poisson's ratio, and Young's modulus. The kriging

College of Mechanical and Electrical Engineering, Sichuan Agricultural University, Ya'an 625014, China. ✉email: 2022217004@stu.sicau.edu.cn

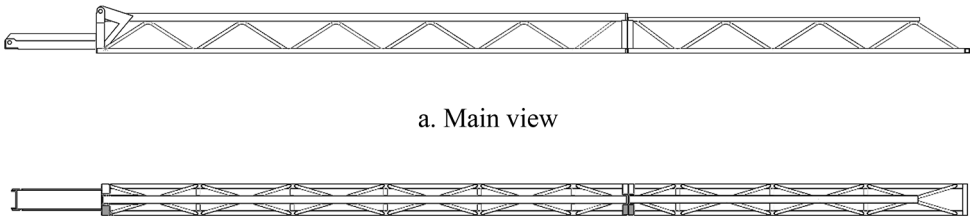

a. Main view

b. Top view

Fig. 1. Model diagram of spray boom truss.

1. Spray boom truss 2.Accelerometer 3.Bungee cord 4.Computer 5. Dynamic Data Collector 6. Force hammer

Fig. 2. Test layout site.

method is then used to construct a response surface model. Using the experimental modal parameters as a standard, the MOGA algorithm is employed to optimize the density, Poisson's ratio, and elastic modulus of the spray boom. Subsequently, sensitivity analysis is conducted to obtain the optimal material parameters. The maximum relative error in modal frequency is calculated, and a comparison is made with the response surface method. Finally, the 7th, 8th, and 9th order natural frequencies and mode shapes of experimental and simulated modes are compared to validate the accuracy improvement of the finite element model of the spray boom for the sprayer.

Methods

Modal test plan of spray boom truss

The truss-type spray boom model studied in this article is shown in Fig. 1. This truss-type spray boom is fabricated by welding multiple square and bent pipes. To enhance stability and strength, the overall structure is processed into a triangular spatial truss. The overall dimensions of the truss are 3300 mm × 188 mm × 170 mm.

The modal testing equipment used in this experiment includes an excitation force hammer, DHDAS testing and analysis software, IMC triaxial acceleration sensor, dynamic data collector, computer, and elastic ropes. Single-point excitation and multi-point pickup vibration are employed to collect modal data. The spray boom truss is dynamically excited by striking it with a force hammer, and the truss's response is recorded using a dynamic data collector. In this experiment, an elastic rope is used to suspend the spray boom truss in mid-air for free modal analysis, as depicted in Fig. 2. A total of 58 measurement points are arranged, and the model structure is drawn in the DHDAS testing and analysis software, as shown in Fig. 3. Acceleration sensors are sequentially placed at the measurement points on the truss. To better excite more modes, the force hammer is applied vertically to the truss between points 37 and 23, and three effective averages are performed. The acceleration sensors record the truss's vibration response under excitation.

Analysis of modal test

The PolyLSCF (Least-Squares Complex Frequency-Domain method) algorithm[20] is a multi-reference point least squares method in the complex frequency domain. It employs a discrete time–frequency domain model, falls

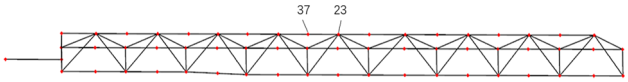

Fig. 3. Test the distribution points.

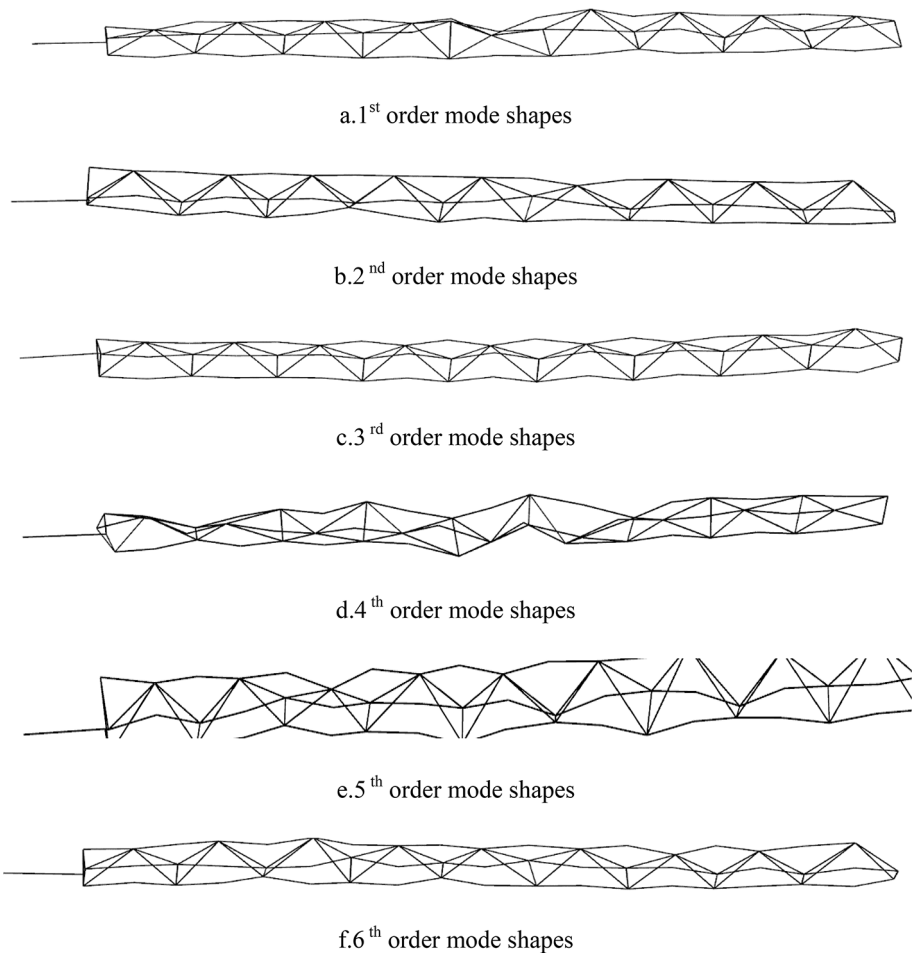

Fig. 4. Experimental mode shape diagram.

under the category of global fitting methods, and is considered the optimal modal parameter identification method in the frequency domain. The PolyLSCF method is suitable for both Experimental Modal Analysis (EMA) and Operational Modal Analysis (OMA), and it supports Multiple Input Multiple Output (MIMO) modal testing. It extracts the first six modal frequencies and mode shapes from the experimental results, as shown in Fig. 4.

A common method for assessing the quality of experimental modal data is through the use of the Model Assurance Criterion (MAC)[21]. This criterion is employed to evaluate the correlation in the vector space (geometry) of modal shapes. The MAC matrix can be expressed as:

$$0 \leq MAC = \frac{\left|\Phi_i^T \Phi_j\right|^2}{(\Phi_i^T \Phi_{\mathrm{i}})(\Phi_j^T \Phi_j)} \leq 1 \tag{1}$$

where Φ_{i} and Φ_j represent the mode shapes of the i-th and j-th modes, respectively.

A MAC value of 0 indicates that the corresponding mode shapes are linearly independent, while a MAC value of 1 indicates that they are linearly correlated. Therefore, an ideal MAC matrix should have diagonal elements close to 1 and off-diagonal elements close to 0. For the mode shape correlation coefficients in the current experiment, as shown in Table 1 and Fig. 5, the MAC matrix appears to be ideal. This suggests that the experimental setup is reasonable, the sensor configuration is effective, and no false modes are present.

MAC	Frequency /(Hz)	First-order modalities	Second-order modalities	Third-order modalities	Fourth-order modality	Fifth-order modalities	Sixth-order modalities
First-order modalities	27.394	1	0	0	0.01	0.06	0
Second-order modalities	41.518	0	1	0.03	0.02	0.01	0.01
Third-order modalities	60.436	0	0.03	1	0.04	0.03	0
Fourth-order modality	69.317	0.01	0.02	0.04	1	0	0
Fifth-order modalities	107.088	0.06	0.01	0.03	0	1	0.01
Sixth-order modalities	115.704	0	0.01	0	0	0.01	1

Table 1. MAC matrix.

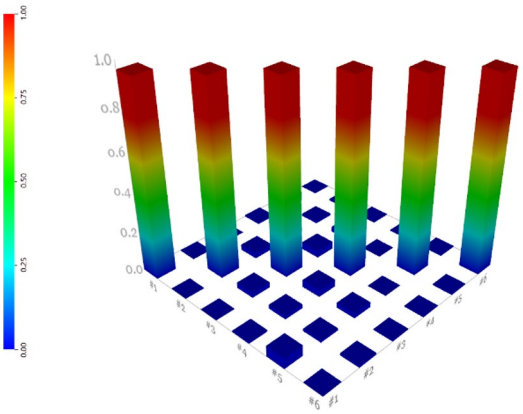

Fig. 5. Experimental modal MAC matrix.

Fig. 6. Finite element model meshing.

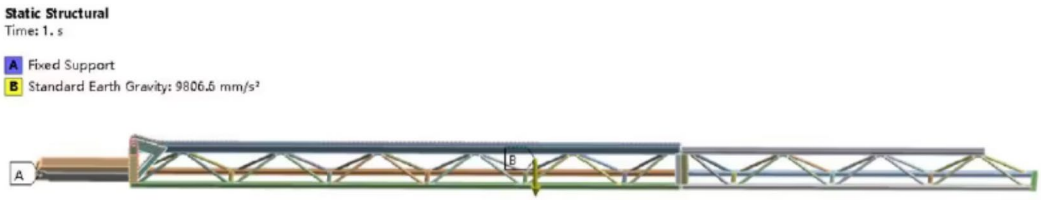

Fig. 7. boundary conditions.

The finite element model of the spray boom truss

In this experiment, modal extraction was performed using the Ansys Workbench18.0 finite element simulation software. A three-dimensional model was created using SolidWorks and imported into Ansys Workbench18.0 as a.x_t file. Material properties were defined within Ansys for the spray boom truss, utilizing structural steel with a density of 7850 kg/m^3, a Poisson's ratio of 0.3, and a Young's modulus of 200,000 MPa. The main mesh size was set to 15 mm, with refinement in specific local regions. A total of 271,192 elements and 554,365 nodes were generated, with a mesh element quality of 0.82, as illustrated in Fig. 6. To obtain a more accurate solution, a mesh convergence analysis was conducted using the Convergence tool under equivalent stress in the static analysis module. The boundary conditions are shown in Fig. 7. The convergence judgment results are shown in Table 2. As can be seen from Table 2, although the number of meshes and nodes increased by 2 to 3 times, the equivalent stress had already tended to stabilize, indicating that the mesh division had achieved a convergent and stable solution.

Serial number	Equivalent stress (MPa)	Change (%)	Nodes	Element
1	126.3	–	554,365	271,192
2	126.84	0.43138	1,325,492	662,359

Table 2. Convergence judgment results.

Analysis of simulation test

In the Ansys Workbench18.0 simulation software, the Lanczos method algorithm was employed to extract the first six non-zero modes, as depicted in Fig. 8.

The experimental and simulated mode shapes were normalized and their degrees of freedom were matched. The relative errors between simulation and experiment were calculated and are presented in Table 3. As shown in Table 3, the relative errors for the 1st and 3rd modes are 8.736% and 7.386%, respectively, indicating significant errors. The relative error for the 2nd mode is even higher at 11.932%, exceeding an acceptable range. This suggests that the current finite element model cannot provide effective guidance. Consequently, updating to the model are necessary.

Finite element model updating of spray boom truss

The objective of model updating is to obtain a finite element model that can reliably predict the mechanical dynamic characteristics. The overall strategy for updating the spray boom truss in this experiment is outlined in Fig. 9.

Finite element model updating involves exchanging data between each step of the updating process and the finite element program. The matrix model obtained by using the physical parameters of the finite element model as updating parameters can easily provide physically meaningful interpretations[22]. In practical applications, material parameters are often within a certain range. The parameter updating method is applied to adjust material parameters, such as density, elastic modulus, Poisson's ratio, bending, and rotational inertia. Therefore, in this study, the parameter updating method will be employed to adjust material density, Poisson's ratio, and Young's modulus.

The traditional approach to updating physical parameters involves repeatedly invoking finite element model iteration calculations, which undoubtedly significantly increases computational load. In order to effectively reduce the number of experiments and shorten the computation time while considering multiple factors comprehensively, this study employs a response surface fitting surrogate model for experimentation.

Experimental design

For material density, Poisson's ratio, and Young's modulus, a range of values is defined. A response surface central composite experimental design with three factors and five levels was employed to set sample points. The values for updating parameters are presented in Table 4, and the experimental design plan is outlined in Table 5.

Kriging model[23] is a regression algorithm based on covariance functions for spatial modeling and prediction (interpolation) of random processes/random fields. Its output is equal to a second-order polynomial (describing the overall behavior of the model) plus a updating term (describing the local behavior of the model). The model can be refined by inserting design points. Using the Kriging model to construct a response surface surrogate model avoids repetitive computations of the model, greatly reducing the computational process. The response surface can be expressed as:

$$\mathrm{y}(x) = \mathrm{g}(x)^T \lambda + z(x) \tag{2}$$

where $\mathrm{y}(x)$ represents the response value; $\mathrm{g}(x)$ is a polynomial function; λ represents the model's basis function; $z(x)$ is a random process with a variance of σ^2 and a mean of 0.

For given initial sample points $X = (x_1, x_2, \cdots, x_n)$ and response values $Y = (y_1, y_2, \cdots, y_n)$, the predicted values and variance of the Kriging model can be expressed as:

$$\hat{\mathrm{y}}(x) = \mathrm{c}(x)^T Y \tag{3}$$

$$MSE = E(\mathrm{c}(x)^T Y - \mathrm{y}(x))^2 \tag{4}$$

where $\mathrm{C}(x)$ represents the response value weight coefficients, and $\hat{\mathrm{y}}(x)$ is the predicted response value for the Kriging sample points.

The accuracy of the response surface model is evaluated using the coefficient of determination R_2. The coefficient of determination R_2 ranges from 0 to 1, with values closer to 1 indicating higher precision of the surrogate model. In this study, there are a total of 15 design points, and the accuracy of the surrogate model is shown in Fig. 10.

MOGA multi-target parameter updating

The MOGA algorithm[24] is a variant based on the Non-dominated Sorting Genetic Algorithm II (NSGA-II). It continuously iterates through processes such as population construction, objective solution, and objective optimization until it finds the optimal values. The MOGA algorithm is employed for optimization. Its mathematical optimization model can be represented as:

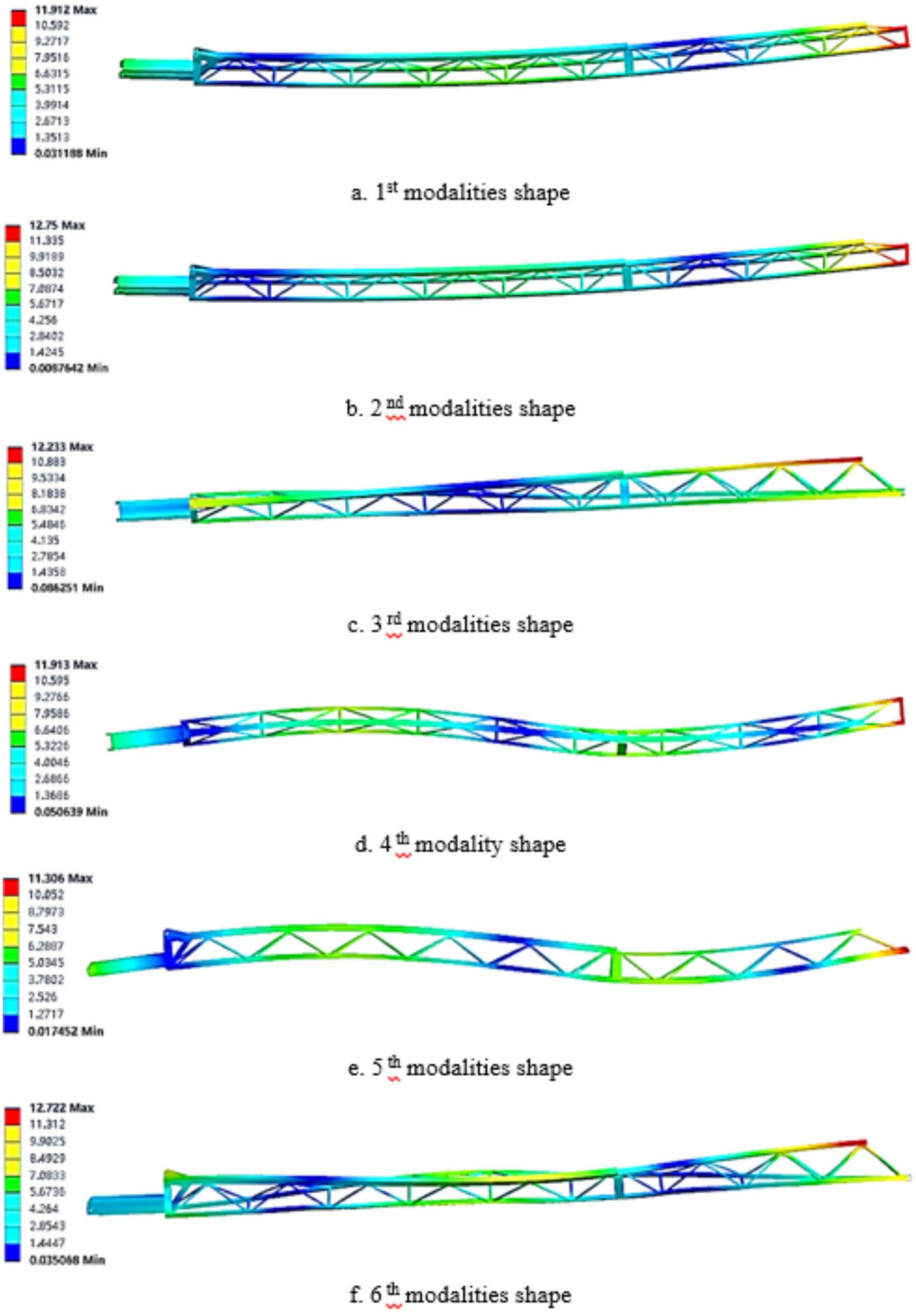

Fig. 8. Mode shape diagram of finite element simulation.

Order	Experimental modal frequency /(Hz)	Simulate modal frequencies /(Hz)	Relative error %
First-order modalities	27.394	29.787	8.736
Second-order modalities	41.518	46.472	11.932
Third-order modalities	60.436	64.9	7.386
Fourth-order modalities	69.317	69.429	0.161
Fifth-order modalities	107.088	111.79	4.391
Sixth-order modalities	115.704	119.22	3.039

Table 3. Table of relative error between test and simulation modes.

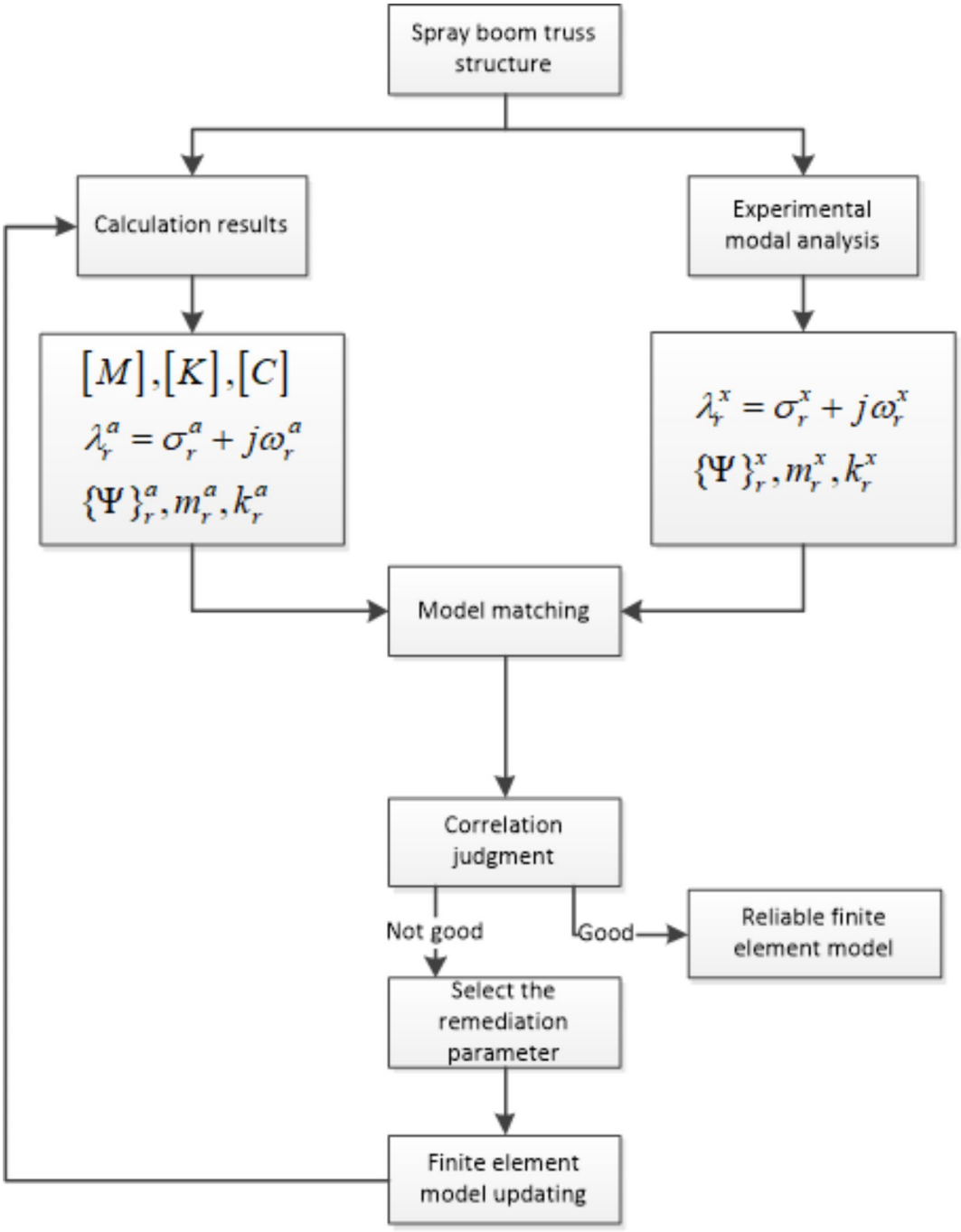

Fig. 9. Flowchart of finite element updating of spray boom truss.

Material Attributes	− 2	− 1	0	1	2
Density (kg/m^3)	6529.79	7065	7850	8635	9170.21
Young's modulus (MPa)	166,364	180,000	200,000	220,000	233,636
Poisson's ratio	0.27	0.285	0.3	0.318	0.33

Table 4. Values of finite element updating parameters.

parameter	Density (kg/m^3)	Young's modulus (MPa)	Poisson's ratio
1	-2	0	0
2	0	0	2
3	-1	-1	1
4	0	0	-2
5	2	0	0
6	1	-1	1
7	0	-2	0
8	0	2	0
9	-1	1	-1
10	-1	-1	-1
11	0	0	0
12	1	1	-1
13	-1	1	1
14	1	-1	-1
15	1	1	1

Table 5. Finite element updating test code table.

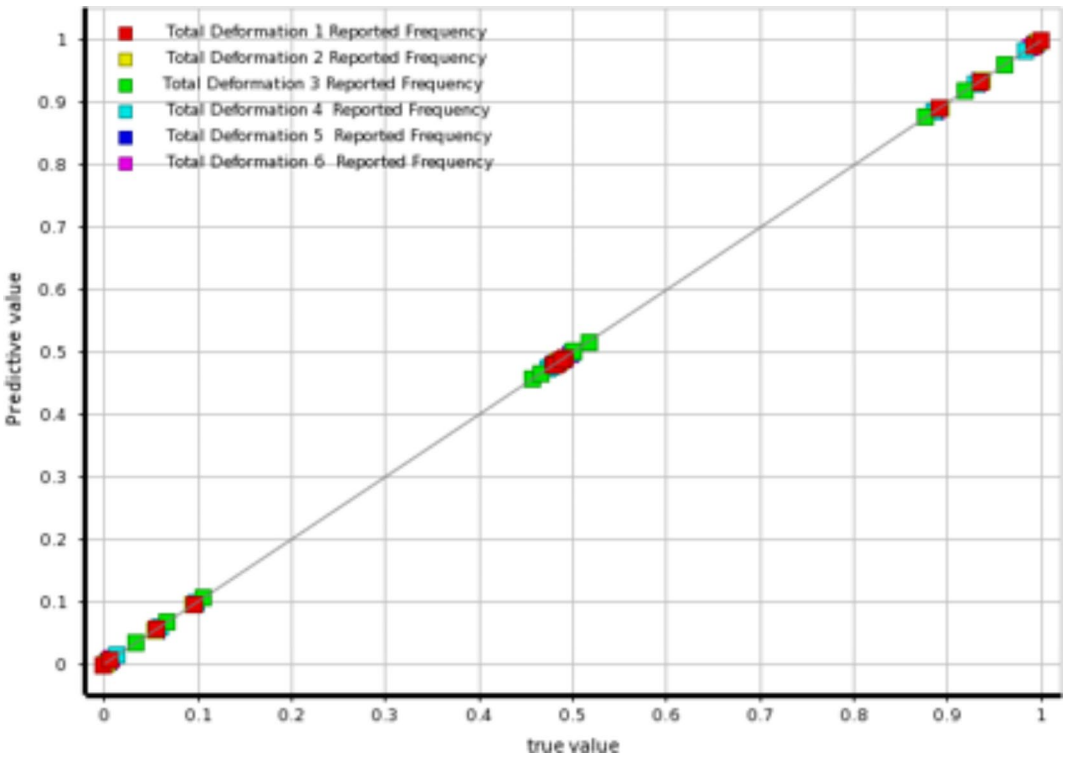

Fig. 10. Surrogate model accuracy.

Material Attributes	Initial parameters	Updated parameters
Density (kg/m^3)	7850	8208.7
Young's modulus (MPa)	200,000	184,280
Poisson's ratio	0.3	0.33

Table 6. Comparison of material parameters.

Order	Experimental modal frequency /(Hz)	Modal frequency after updating /(Hz)	Relative error (%)
First-order modalities	27.394	27.984	2.154
Second-order modalities	41.518	43.332	4.369
Third-order modalities	60.436	60.731	0.488
Fourth-order modalities	69.317	66.126	4.603
Fifth-order modality	107.088	104.98	1.968
Sixth-order modalities	115.704	112.12	3.098

Table 7. Updating results and relative errors of the response surface method.

$$\begin{gathered}\left(\sum_{i=1}^{m}\left|f_i(x)-y_i\right|\right)_{\min} \\ s.t.\ \rho_1 \leq \rho \leq \rho_u \\ \mathrm{E}_1 \leq \mathrm{E} \leq E_u \\ \nu_1 \leq \nu \leq \nu_u\end{gathered} \tag{5}$$

where m represents the number of objective functions, $f(x)$ represents the objective functions, y represents the objective values, and ρ, E, ν respectively represent density, Young's modulus, and Poisson's ratio.

A total of 1000 initial samples were set, and the sample size for each iteration was set to 20. The search results were required to have frequency errors between calculated modes and experimental modes not exceeding 5%. The final updated material parameters are presented in Table 6, and the updating results are shown in Table 7. From the updating results, it can be observed that the relative errors for the second and fourth modes are 4.369% and 4.603%, respectively, indicating relatively large errors. The iteration curves for the search points of the second and fourth mode frequencies are depicted in Fig. 11. It can be seen that, although the algorithm can find optimal values during iteration, the MOGA algorithm comprehensively selects the overall optimal value when considering multiple constraint objectives.

To improve computational efficiency, sensitivity analysis is performed on the finite element model using the Spearman correlation coefficient[25]. The correlation coefficient ρ can be expressed as:

$$\rho = \frac{\sum_{i=1}^{\mathrm{n}}(x_i-\overline{x})(y_i-\overline{y})}{\sqrt{\sum_{i=1}^{\mathrm{n}}(x_i-\overline{x})^2\sum_{i=1}^{n}(y_i-\overline{y})^2}} \tag{6}$$

where x_i and y_i are the ranking values of sample point i, $\overline{x}$ and $\overline{y}$ are the average rankings of x and y, and n is the number of sample points.

The correlation between optimization objectives and material properties is shown in Fig. 12. From the figure, it can be observed that density is negatively correlated with frequency, Young's modulus is positively correlated with frequency, and Poisson's ratio has a relatively small impact. Therefore, based on the response surface method, Poisson's ratio is set to 0.33, and then parameter updating is performed again.

Finally, the results of the finite element model after sensitivity analysis updating are presented in Table 8. The maximum relative error of modal natural frequencies for the finite element model updated based on sensitivity analysis is reduced to 4.961%. The results indicate that the parameter updating based on sensitivity analysis meets engineering requirements, while computational efficiency has increased. However, the accuracy is slightly lower compared to the response surface method.

Model validation

To verify the credibility of the finite element model after updating, the unmodified 7th, 8th, and 9th order natural frequencies and mode shapes are compared with the experimental modal frequencies and mode shapes. The material parameters of the finite element model are adjusted to the parameters updated by the response surface method. Calculations are carried out under the previous conditions, and the first 9 non-zero free modal

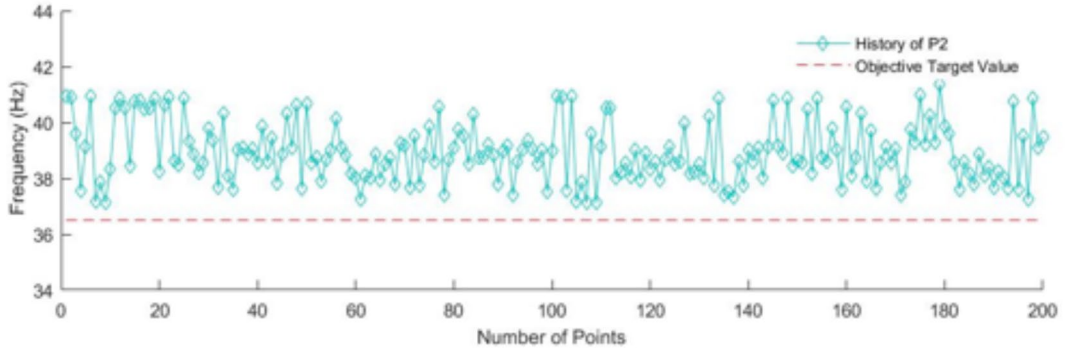

a. Second-order frequency search curve

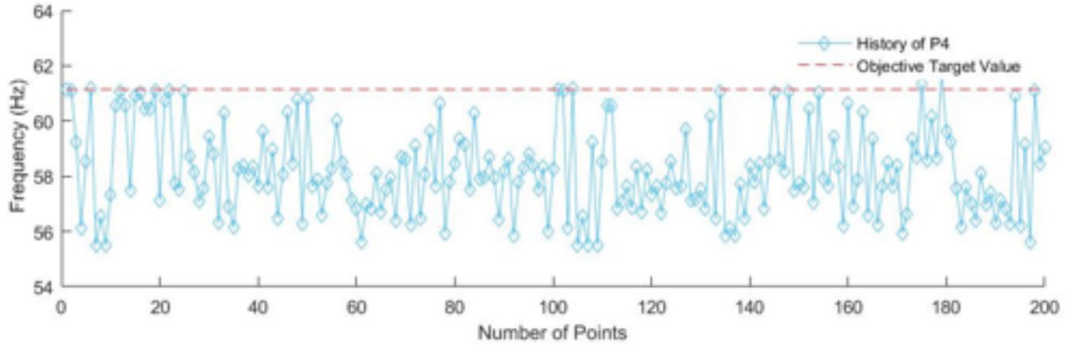

b. Fourth-order frequency search curve

Fig. 11. MOGA algorithm search curve.

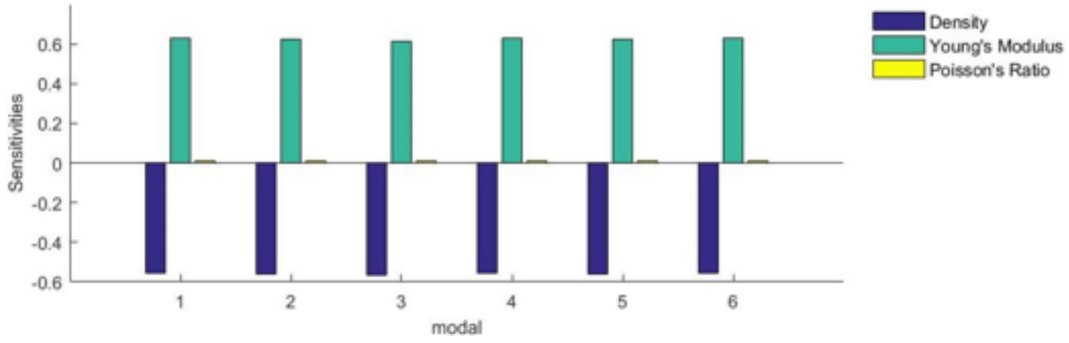

Fig. 12. Updating of material properties.

frequencies are extracted, as shown in Table 9. The relative errors are 2.323%, 3.716%, and 5.137%, respectively, all within the permissible error range for engineering. The mode shapes also exhibit high consistency. It can be concluded that the finite element updated model reflects the actual dynamic characteristics of the structure well and can provide correct guidance for practical engineering.

Results

This article provides a detailed study through modal testing and finite element simulation of the spray boom truss, focusing on the updating of material parameters in the finite element model to enhance its credibility. The specific summary of the work is as follows:

Order	Experimental modal frequency /(Hz)	Experimental modal frequency /(Hz)	Relative error (%)
First-order modalities	27.394	28.312	3.35
Second-order modalities	41.518	43.578	4.961
Third-order modalities	60.436	60.64	0.338
Fourth-order modalities	69.317	65.925	4.893
Fifth-order modality	107.088	104.757	2.177
Sixth-order modalities	115.704	111.826	3.352

Table 8. Relative error after updating for the sensitivity method.

Order	Experimental modal frequency /(Hz)	Experimental modal frequency /(Hz)	Relative error (%)
Seventh-order modality	133.391	136.49	2.323
Eighth-order modalities	174.794	181.29	3.716
Ninth-order modalities	211.389	200.53	5.137

Table 9. Validation table.

1. Modal parameters of the spray boom were obtained through experimental testing. The rationality of the experimental arrangement and the reliability of modal testing were verified through modal assurance criteria.
2. A response surface model was constructed using the kriging method. In response to a maximum relative error of 11.93% in the first six non-zero modal frequencies between finite element simulation and actual experiments, updating were made to the finite element model. The MOGA algorithm was employed for multi-objective parameter updating, optimizing density, Young's modulus, and Poisson's ratio. After optimization, with density at 8208.7 kg/m^3, Young's modulus at 184,280 MPa, and Poisson's ratio at 0.33, the maximum relative error in natural frequencies was reduced to 4.603%. To seek a more efficient updating method, sensitivity analysis was further performed to identify a low-sensitivity Poisson's ratio (fixed at 0.33). The same optimization steps were then repeated, resulting in a final maximum relative error of 4.961%. The results indicate higher accuracy with the response surface method, while the sensitivity method exhibits faster computational speed. Both methods effectively improved the relative error of the updated finite element model in modal frequencies compared to experimental results, enhancing the model's accuracy.
3. The updated parameters were applied to the original finite element model for modal extraction. The seventh, eighth, and ninth-order natural frequencies and mode shapes from both simulation and experiment were compared, ultimately validating the credibility of the finite element model.

Discussion

In this study, the material parameters of the finite element model of the truss structure were updated using the response surface method and the sensitivity method. Each method has its advantages and disadvantages, but compared to previous studies, both methods can effectively improve the accuracy of the finite element model. Additionally, the finite element model correction method proposed in this study is applicable to various similar truss structures, providing a beneficial research foundation for the simulation analysis of truss structures. The model, with improved accuracy based on this method, will be used in the future to provide valuable information to engineers, improve data quality, and reduce testing time. It will be primarily used for dynamic simulation, static analysis, lightweight design, optimization design, and other related tasks. Currently, the corrected finite element model of the truss has been applied to simulation optimization in lightweight and vibration reduction, and it has been found that the mechanical performance of the optimized truss structure has been significantly improved.

Data availability

The data that support the findings of this study are available on request from the corresponding author, Lihua Zhang, upon reasonable request.

Received: 2 April 2024; Accepted: 19 September 2024
Published online: 01 October 2024

References

1. Li, J., Shi, Y., Lan, Y. & Guo, S. Vertical distribution and vortex structure of rotor wind field under the influence of rice canopy. *Comput. Electron. Agric.* **159**, 140–146. https://doi.org/10.1016/j.compag.2019.02.027 (2019).
2. Xu, D. et al. Effects of spray parameters on pesticide utilization efficiency and droplet deposition distribution in paddy field of self-propelled boom sprayer. *Chin. J. Pestic. Sci.* **22**, 324–332 (2020).
3. Ramon, H. & De Baerdemaeker, J. Spray boom motions and spray distribution: Part 1, derivation of a mathematical relation. *J. Agric. Eng. Res.* **66**, 23–29. https://doi.org/10.1006/jaer.1996.0114 (1997).
4. Ramon, H., Missotten, B. & De Baerdemaeker, J. Spray boom motions and spray distribution: Part 2, experimental validation of the mathematical relation and simulation results. *J. Agric. Eng. Res.* **66**, 31–39. https://doi.org/10.1006/jaer.1996.0115 (1997).

5. Lee, J. Free vibration analysis of joined conical-cylindrical shells by matched Fourier-Chebyshev collocation method. *J. Mech. Sci. Technol.* **32**, 4601–4612. https://doi.org/10.1007/s12206-018-0907-0 (2018).
6. Zhang, H., Li, D. & Li, H. Recent progress on finite element model updating: From linearity to nonlinearity. *Adv. Mech.* **49**, 542–575. https://doi.org/10.6052/1000-0992-18-004 (2019).
7. Shi, J., Wu, Q., Guo, W., Yang, X. & Huang, Y. Application of modal effective mass for finite element model construction. *J. Syst. Simul.* **25**, 995–998. https://doi.org/10.16182/j.cnki.joss.2013.05.036 (2013).
8. Liu, G. *et al.* A finite element model updating method based on improved MCMC method. *Eng. Mech.* **33**, 138–145. https://doi.org/10.6052/j.issn.1000-4750.2014.10.0887 (2016).
9. Mottershead, J. E. & Friswell, M. I. Model updating in structural dynamics: A survey. *J. Sound Vib.* **167**, 347–375. https://doi.org/10.1006/jsvi.1993.1340 (1993).
10. Baklanov, V. S. Low-frequency vibroisolation mounting of power plants for new-generation airplanes with engines of extra-high bypass ratio. *J. Sound Vib.* **308**, 709–720. https://doi.org/10.1016/j.jsv.2007.04.042 (2009).
11. Xu, X. et al. Full flexible model updating of single-strip pantograph based on modal test. *Chin. J. Theor. Appl. Mech.* **55**, 1–8. https://doi.org/10.6052/0459-1879-23-063 (2023).
12. He, H., Cao, X., Xu, H. & Hou, S. Modal test and model modification of spiral bevel gears. *J. Aerosp. Power* **38**, 1–9. https://doi.org/10.13224/j.cnki.jasp.20220978 (2023).
13. Liu, G., Chen, Q., Lei, Z. & Xiong, J. Finite element model updating method based on improved firefly algorithm. *Eng. Mech.* **39**, 1–9. https://doi.org/10.6052/j.issn.1000-4750.2021.04.0271 (2022).
14. Li, J. & Xu, F. Finite element model updating based on kriging model and MOGA algorithm. *Adv. Aeronaut. Sci. Eng.* **14**, 68–75. https://doi.org/10.16615/j.cnki.1674-8190.2023.04.07 (2023).
15. Zhang, X., Peng, Z. & Zhang, Y. Stochastic finite element model updating based on kriging model and improved MCMC algorithm. *Chin. J. Comput. Mech.* **38**, 712–721. https://doi.org/10.7511/jslx20201019001 (2021).
16. Su, Z., Han, D. & Cui, Z. Helicopter rotor blade model updating method based on sensitivity analysis. *J. Aerosp. Power* **38**, 1–8. https://doi.org/10.13224/j.cnki.jasp.20220869 (2023).
17. Liu, L., Li, F., Song, Y., Liu, C. & Wu, P. Finite element model updating of bogie frame based on sensitivity analysis. *J. Vib. Shock* **42**, 181–186. https://doi.org/10.3465/j.cnki.jvs.2023.03.021 (2023).
18. Zhang, Q., Zhu, Y., Zhao, Y. & Yang,. Finite element model updating method of diesel engine airframe based on sensitivity analysis. *Ship Eng.* **44**, 87–91. https://doi.org/10.13788/j.cnki.cbgc.2022.12.14 (2022).
19. Mottershead, J. E., Link, M. & Friswell, M. I. The sensitivity method in finite element model updating: A tutorial. *Mech. Syst. Signal Process.* **25**, 2275–2296. https://doi.org/10.1016/j.ymssp.2010.10.012 (2011).
20. Culla, A., D'Ambrogio, W., & Fregolent, A. Getting a symmetric residue matrix from the poly-reference least square complex frequency domain technique. In *Proceedings of the Proceedings of ISMA 2755-2764* (2012).
21. Li, D. & Lu, Q. *Experimental Modal Analysis and Its Applications* (Science Press, 2001).
22. Weng, S. & Zhu, H. Damage identification of civil structures based on finite element model updating. *Eng. Mech.* **38**, 1–16. https://doi.org/10.6052/j.issn.1000-4750.2020.06.ST02 (2021).
23. Stein, M. L. *Interpolation of Spatial Data: Some Theory for Kriging* (Springer, 2012).
24. Murata, T., & Ishibuchi, H. MOGA: Multi-objective genetic algorithms. In *Proceedings of the IEEE International Conference on Evolutionary Computation* vol 1, 289–294 ((1995)). https://doi.org/10.1109/ICEC.1995.489161
25. Wissler, C. The Spearman correlation formula. *Science* **22**, 309–311. https://doi.org/10.1126/science.22.558.30 (1905).

Acknowledgements

Conceptualization, L.Z. and Q.C.; methodology, Q.C.; software, Q.C. and S.Z.; validation, Q.C., Y.Z., Y.X. and L.C.; formal analysis, L.Z.; investigation, L.Z. and Q.C.; resources, Q.C.; data curation, Q.C.; writing—original draft preparation, Q.C.; writing—review and editing, Q.C., S.Z., Y.X., L.C., Y.Z. and L.Z.; funding acquisition, Y.Z. All authors have read and agreed to the published version of the manuscript.

Author contributions

Conceptualization, L.Z. and Q.C.; methodology, Q.C.; software, Q.C. and S.Z.; validation, Q.C., Y.Z., Y.X. and L.C.; formal analysis, L.Z.; investigation, L.Z. and Q.C.; resources, Q.C.; data curation, Q.C.; writing—original draft preparation, Q.C.; writing—review and editing, Q.C., S.Z., Y.X., L.C., Y.Z. and L.Z.; funding acquisition, Y.Z. All authors have read and agreed to the published version of the manuscript.

Funding

This research was funded by the National Key Research and Development Program of China (2022YFD2300903-2) and the National Industry System of Corn Technology (CARS-02).

Declarations

Competing interests

The authors declare no conflict of interest.

Additional information

Correspondence and requests for materials should be addressed to L.Z.

Reprints and permissions information is available at www.nature.com/reprints.

Publisher's note Springer Nature remains neutral with regard to jurisdictional claims in published maps and institutional affiliations.